Global NEST Journal, Vol 26, No X, pp 1-8

Removal of gaseous ammonia released from leachate by adsorption on carbon-based adsorbents prepared from agro-industrial wastes

Thalles Perdigão-Lima[1,2], Jose L. Diaz De Tuesta[1,3]*, Manuel Feliciano[1,2,]*, Leonardo Campestrini Furst[1,2], Fernanda F. Roman[1,2,5], Adriano S. Silva[1,2,5], Adriana A. Pereira Wilken[4], Adrián M.T. Silva[5] and Helder T. Gomes[1,2]

[1]Centro de Investigação de Montanha (CIMO), Instituto Politécnico de Bragança, Campus de Santa Apolónia, 5300-253 Bragança, Portugal

[2]Laboratório Associado para a Sustentabilidade e Tecnologia em Regiões de Montanha (SusTEC), Instituto Politécnico de Bragança, Campus de Santa Apolónia, 5300-253 Bragança, Portugal

[3]Chemical and Environmental Engineering Group, ESCET, Rey Juan Carlos University, C/Tulipán S/N, 28933 Móstoles (Madrid), Spain

[4]Departamento de Ciência e Tecnologia Ambiental do Centro Federal de Educação Tecnológica de Minas Gerais, Brazil;[5] Laboratory of Separation and Reaction Engineering - Laboratory of Catalysis and Materials (LSRE-LCM), Faculdade de Engenharia, Universidade do Porto, Rua Dr. Roberto Frias, 4200-465 Porto, Portugal.

Received: 12/03/2023, Accepted: 13/01/2024, Available online: 25/02/2024

*to whom all correspondence should be addressed: e-mail: jl.diazdetuesta@ipb.pt, msabenca@ipb.pt

https://doi.org/10.30955/gnj.004862

Graphical abstract

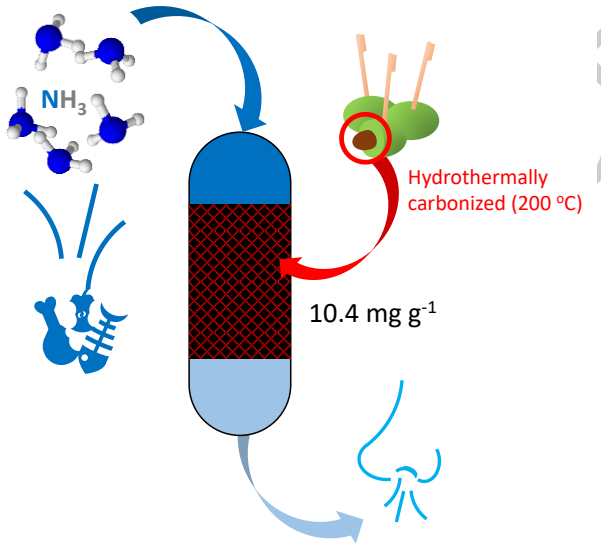

Abstract

Landfill facilities and organic waste treatment plants typically are known sources of odour pollution, such as gaseous NH_3, among others. In this work, the removal of gaseous NH_3 released from a composting line of a mechanical and biological treatment plant of undifferentiated municipal solid waste was assessed in a fixed-bed column loaded with carbon-based adsorbents (CBAs) prepared from olive stone and malt bagasse as carbon precursors. CBAs were prepared by hydrothermal carbonization (HTC) assisted by H_2SO_4 and pyrolysis, resulting in materials with different physical and chemical properties. The hydrochar derived from olive stone by H_2SO_4-assisted HTC was found as the best adsorbent for NH_3 removal (10.4 mg g^{-1}). This result was ascribed to the high acid character of the adsorbent (2.34 mmol g^{-1}), since it was found that acidity contributed significantly more than the specific surface of the adsorbents for the removal of NH_3 (BET surface of 4 m^2 g^{-1} was obtained for the CBA with the highest uptake capacity, whereas other adsorbents reach values of 172 m^2 g^{-1} and NH_3 uptake capacities of 0.07 mg g^{-1}). The NH_3-saturated hydrochar was regenerated by washing with water and subsequently reused in the adsorption of NH_3, with a performance more than 70% compared to its first use.

Keywords: Valorisation; Biomass; Hydrothermal Carbonization; Pyrochars; Acid Adsorbents; Air Pollution; Odour Contamination; Circular Economy; Municipal Solid Waste.

1. Introduction

Odour pollution can cause adverse effects in humans, including various undesirable reactions, ranging from annoyance to documented health effects (Nicell 2009). Odorous pollutants may result directly or indirectly from human activities, such as waste treatment plants. Despite contributing to proper waste management, landfill facilities and compost plants are normally sources of odour pollution (Rincón *et al.* 2019). Gaseous ammonia (NH_3) is one of the priority odorants detected in both landfill facilities and composting plants and should be taken into consideration on health risk assessment (Cheng *et al.* 2019). Adsorption may be used for its removal, since the process has been successfully employed to remove inorganic and organic pollutants in the environment in general, including odorous ones (Dai *et al.* 2018).

The removal of NH_3 requires the development of suitable and low-cost adsorbents for its uptake. In this sense,

carbon-based adsorbents (CBAs) have demonstrated high flexibility and performance since carbon materials may be produced by various ways to form linear, planar and tetrahedral bonding arrangements with a large range of properties (surface area, porosity and surface chemistry) for selected applications (Bi *et al.* 2019; Roman *et al.* 2021a; Vieira *et al.* 2022). Some examples of CBAs are pyrochars and hydrochars. Pyrochars are the solid char remaining from one-step thermal decomposition (<900ºC and oxygen-limited atmosphere) of a carbon source and present high porosity development (Zhang *et al.* 2019). Hydrochars are carbonaceous materials prepared by hydrothermal carbonization (HTC), a thermo-chemical process, which uses water, heat (<400ºC) and high pressure (Diaz de Tuesta *et al.* 2021a; de Freitas Batista *et al.*,2022). More novelty approaches consist in the use of catalyst and chemical agents in HTC to modify hydrochar's properties and improve their performance (Diaz de Tuesta *et al.* 2021a; Susanti *et al.* 2019).

One of the most attractive advantages of CBAs is the wide carbon sources available for their production, such as biomass (Bi *et al.* 2019), plastic wastes (Vieira *et al.* 2022), fertilizers (Roman *et al.* 2021b) or other low-cost sources that allow the production of CBAs with a low price (Hadi el al. 2015; Basso *et al.* 2015). In this sense, biomass residues coming from agro-industrial explorations result in an attractive renewable carbon source to be converted into CBA (Mohamed *et al.* 2010). In addition, the conversion of this inexhaustible, low-cost and non-hazardous biomass into CBAs is an appropriate destination of the biomass residue produced in agro-industrial activities (Diaz de Tuesta *et al.* 2021a). For this reason, the valorisation of biomass as precursors of CBAs is a practical strategy to increase resource-use efficiency by simultaneously reducing the environmental waste burden and achieving the effect of "treating pollution with waste". In addition, it keeps natural resources in use for as long as possible, which is the principle of the circular economy (Baldikova *et al.* 2019).

This work aims at the preparation of CBAs, viz. hydrochars and pyrochars, using olive stone and malt bagasse as feedstocks, and further evaluation of its performance and effectiveness in the adsorption of the odorous pollutant NH_3 by using a fixed-bed column. For this purpose, adsorption runs were conducted using NH_3, deriving from leachate waters originated from a composting line of a mechanical and biological treatment plant of municipal solid wastes.

2. Experimental methods

2.1. Reagents and materials

A leachate sample was obtained from a leachate storage tank at a plant of the company Resíduos do Nordeste, EIM (Mirandela, Portugal). Olive stones (OS) and malt bagasse (BM) were supplied by Brazilian agro industries from the state of Paraná. Sulfuric acid (H_2SO_4, 98%), used as a chemical agent in the HTC process, was supplied by LabKem, whereas for carbonization, nitrogen (N_2, X4) from Air Liquide was used. 37% hydrochloric acid (HCl) and 98% sodium hydroxide (NaOH) were obtained from Fisher chemical. Phenolphthalein was supplied by Riedel-de-Häen. All reagents were used as received, without further puri-fication, and distilled water was used throughout the research.

2.2. Preparation of CBAs

Firstly, olive stones and malt bagasse were dried overnight at 60ºC and milled into a centrifugal mill (model Retsch Ultra ZM 200) using a ring sieve with trapezoid holes of 0.25 mm, resulting in OS and MB adsorbents, respectively. Then, OS and MB were pyrolyzed to produce OS-P and MB-P pyrochars, respectively. Pyrolysis was conducted in a quartz tubular furnace (Thermconcept) under N_2 continuous flow rate of 100 $Ncm^3\ min^{-1}$ up to 800ºC for 4 h, following the detailed methodology described in previous works (de Freitas Batista *et al.* 2022; Diaz de Tuesta *et al.* 2018).

Additionally, OS-HTC and BM-HTC hydrochars were prepared by H_2SO_4-assisted HTC, according to a method previously described (Diaz de Tuesta *et al.* 2021a; Roman *et al.* 2021b). Briefly, a suspension containing OS or BM (1 $g{\cdot}mL^{-1}$) with 2.5 mol L^{-1} H_2SO_4 was placed into a high-pressure batch reactor (Model 249M 4744-49, Parr Instrument Company) and kept under autogenous pressure at 200ºC for 3 h. After cooling, the hydrochars were recovered by filtration and washed with abundant distilled water. Finally, hydrochars were dried in a drying chamber at 100ºC for 24 h.

2.3. CBAs characterization

Carbon, nitrogen, hydrogen and sulfur content in CBAs was determined by elemental analysis in triplicate using a Carlo Erba EA 1108 Elemental Analyser. Ash content was determined as detailed in previous research papers (Diaz de Tuesta *et al.* 2021b).

The textural properties of the CBAs were determined from the N_2 adsorption–desorption isotherm curves of the adsorbents, obtained at -196ºC in a Quantachrome NOVA TOUCH LX4 analyser. Vacuum degasification was performed for 16 h at 200ºC. Brunauer-Emmett-Teller (BET), external and micropore surface areas (S_{BET}, S_{ext} and S_{mic}, respectively), and the micropore volume (V_{mic}) were quantified by BET and *t*-plot methods. Total pore volume (V_{Total}) was determined for p/p^0 = 0.98. Calculations of those methods were all done by using TouchWinTM software v1.21.

The acidity and basicity of CBAs were quantified by acid-base titration using HCl and NaOH solutions, and phenolphthalein as an indicator, as described elsewhere (Santos Silva *et al.* 2019). Briefly, for the determination of acidity, 0.2 g of each CBA was mixed with 25 mL of a 0.02 M NaOH solution and kept under stirring for 48 h at room temperature. Afterward, each suspension was filtered, and mL of the resultant liquid was titrated with a 0.02 M HCl solution to determine unreacted OH^-. Then, the acidity of each CBA was calculated by the difference between the initial NaOH and the determined amount of NaOH by titration. The determination of the basicity of each CBA was done using 0.02 M HCl as the initial solution and titrating the resultant 20 mL after filtration with 0.02 M NaOH.

2.4. Adsorption of NH_3 on CBAs

A lab-scale system was assembled to run adsorption tests, to evaluate the performance and effectiveness of the prepared adsorbents, similar to those previously reported (Zafanelli *et al.* 2022; Karimi *et al.* 2020).

The adsorption runs were conducted in the setup shown in Figure 1, which consists of: (1) Zero Air Generator (ZAG), (2) Mass Flow Controller (MFC), (3) Gas Wash Bottle (GWB), (4) Fixed-Bed (FB) column, and (5) MultiGas Analyzer (MGA). The ZAG (model SONIMIX 3012) was used to generate an air specially cleaned, whose flow (0.8 mL min^{-1}) was controlled by the MFC (model Brooks 4800 Series) and led to the GWB containing the leachate (5 mL). Then, the NH_3-saturated air was led to the FB column flowing downward through the selected CBA to avoid disturbing the bed (ASTM D5160-95) and the NH_3 concentration was followed by the MGA (model GASERA ONE PULSE).

All adsorption tests were performed at a flow rate of 0.8 L min^{-1}, room temperature and pressure of approximately 93.7 KPa. The FB column was designed based on ASTM D5160-95(19) – Standard Guide for Gas-phase Adsorption Testing of Activated Carbon. It consisted of a vertically supported cylindrical acetate tube (inner diameter = 1.2 cm, height = 8.5 cm) filled with adsorbent and supported at its lower end by a flat fine mesh stainless steel screen to ensure fixed packing of the bed. Another mesh was placed at its upper end to ensure uniformity of flow profile across the adsorbent bed. Inert glass wool was used above and below the adsorbent to avoid slippage.

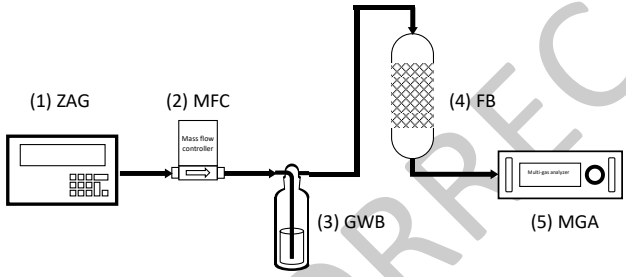

Figure 1. Setup for adsorption runs.

NH_3 concentration of the downstream was measured every 3 min until a few minutes after reaching the saturation of the bed. Blank experiments were conducted with non-CBA bed to determine the initial NH_3 concentration of the inlet flow in the adsorption column coming from the GWB containing leachate.

All NH_3 adsorption experiments on the CBAs were conducted in triplicate, and the breakthrough curves are plotted by smoothening data using the moving average method. Breakthrough time (t_b), saturation time (t_{sat}), height of mass transfer zone (H_{MTZ}) and dynamic adsorption capacity (N_0) were determined from the analysis of breakthrough curves. Breakthrough time (t_b) and saturation time (t_{sat}) were defined considering the first point that presented an increase of NH_3 concentration and as the point that presented 95% of the inlet NH_3 concentration (C/C_0 = 0.95), respectively (Ang *et al.* 2020; Balsamo *et al.* 2013). The height of the mass transfer zone (H_{MTZ}) per height of adsorption bed (Z) was estimated by Eq. (1) (Ang *et al.* 2020).

$$H_{MTZ} / Z = \frac{t_{sat} - t_b}{t_{sat}} \quad (1)$$

where t_b (h) and t_{sat} (h) are breakthrough time and saturation time, respectively.

The dynamic adsorption capacities of each CBA (Q_a, milligrams of adsorbate, *i.e.* NH_3, per grams of CBA) were estimated by integration of the area under the breakthrough curve, also considering the system flow rate and the mass of adsorbent used, as expressed in Eq. (2) (Zafanelli *et al.* 2022; Karimi *et al.* 2020):

$$Q_a = \frac{F}{m} \cdot \int_0^{t_{csat}} (C_0 - C_t)\, dt \quad (2)$$

where F is the gas flow rate (L h^{-1}) of the cleaned air generated, m is the mass of CBA (g), C_0 and C_t are the NH_3 concentrations at the beginning and each time-on-stream, and t_{csat} is the time (h) when the adsorption bed reaches the complete saturation ($C_t = C_0$).

3. Results and discussion

3.1. Composition of CBAs

Table 1 presents the composition weight percentages (%wt) of carbon, hydrogen, nitrogen, sulphur and ash of the CBAs, as well as the remaining content (R.C.) and the mass losses (M.L.) obtained during the preparation of each CBA.

The values of composition weight percentages (%wt) found for OS are close to those found in the literature: 43.1 – 52.3% for C; 5.9 – 7.1% for H; 0.03 - 1.0% for N; 0.01 – 0.8% for S; and 0.37 – 4.4% for ash (Ghouma *et al.* 2015; Martín-Lara *et al.* 2013; Cagnon *et al.* 2009; González *et al.* 2009). The values of composition weight percentages (%wt) found for BM are also similar to results reported in the literature: 46.8% for C; 8.2% for H; 3.9% for N; 0.38% for S; and 2.8% for ash (Franciski *et al.* 2018; Mello and Mali 2014). As observed, the pyrolyzed adsorbents (OS-P and MB-P) show the highest C content (88.0% and 72.5%, respectively) and the lowest H amount (1.0% and 1.3%, respectively) among the adsorbents prepared from the same precursor, hence the highest C/H ratios values (85.3% and 56.1%, respectively). Both (OS-P and MB-P) presented higher values of C content and C/H ratios than their respective feedstocks (49.3% of C and 7.9 of C/H for OS, and 44.9% of C and 6.8 of C/H for MB). The samples prepared by H_2SO_4-assisted HTC (OS-HTC and MB-HTC) also show higher quantities of carbon and values of C/H ratio (74.7% of OS-HTC and 12.8 of C/H for OS-HTC, and 68.1% of C and 11.0 of C/H for MB-HTC). Those results may be related to the decomposition and carbonization reactions, in which organic fractions of the feedstocks may have either been decomposed into volatile matter (e.g., CO, CO_2 and CH_4) and released as gases, or carbonized forming the chars with yielded aromaticity (Chen *et al.* 2017; Lam *et al.* 2017; Yek *et al.* 2019). The matter released during both carbonization processes is evidenced by the mass losses (M.L.) during the preparation of each CBA. At the selected operating conditions, pyrolysis led to the loss of three quarters of the feedstock (74.9% for OS-P from OS and 75.8% for MB-P

from MB), whereas HTC allowed to obtain the highest yields (50.7% and 59.7% of M.L. for OS-HTC and MB-HTC from OS and MB, respectively).

The carbonization processes also affect significantly the ash content of each resultant CBA. The content of ashes in carbon-based materials prepared from biomass is due to the minerals present in the feedstock used, mainly Ca, Mg, Na, K, Fe, Si and Al, among others (Lacey *et al.* 2018; Jahn *et al.* 2020). Pyrolysis led to obtaining pyrochars with a higher ash quantity (4.0% and 11.4% of ashes for OS-P and MB-P, respectively). In contrast, HTC treatment allows decreasing the inorganic matter present in feedstocks (0.6% and 3.2% for OS and MB, respectively), since OS-HTC and MB-HTC show 0.2% and 1.1% of ashes content, respectively. This is ascribed to the release of volatile organic content during the pyrolysis process and the leaching of inorganic matter into the water phase used in HTC. In previous works regarding HTC of seed of chia and sugarcane bagasse, a decrease in the ash content at equal operational conditions was also observed (Diaz de Tuesta *et al.* 2021a): from 2.1-6.4% to 1.1-4.5%, depending on the feedstock precursor. In this work, the leaching was higher due to the acid attack occurring by the presence of H_2SO_4 during HTC.

Table 1. Composition and textural properties of the CBAs.

CBA	C/H	C (wt.%)	H (wt.%)	N (wt.%)	S (wt.%)	Ash (wt.%)	R.C.† (wt.%)	M.L.¥ (%)	S_{BET} (m^2 g^{-1})	S_{mic} (m^2 g^{-1})	V_{Total} (mm^3 g^{-1})
OS-HTC	12.8	74.7 (±1.1)	5.8 (±0.5)	0.1 (±0.1)	0.75 (±0.07)	0.2	18.5	50.7	4	0	16
OS-P	85.3	88.0 (±0.5)	1.0 (±0.1)	1.1 (±0.1)	0.08 (±0.03)	4.0	5.8	74.9	172	158	109
OS	7.9	49.3 (±0.3)	6.3 (±0.2)	0.2 (±0.1)	0.06 (±0.04)	0.6	43.6	-	-	-	-
MB-HTC	11.0	68.1 (±3.3)	6.2 (±0.5)	0.7 (±0.1)	0.77 (±0.05)	1.1	23.1	59.7	12	1	25
MB-P	56.1	72.5 (±1.7)	1.3 (±0.1)	3.3 (±0.3)	0.05 (±0.03)	11.4	11.5	75.8	50	39	34
MB	6.8	44.9 (±0.2)	6.6 (±0.1)	2.4 (±0.6)	0.18 (±0.03)	3.2	42.7	-	-	-	-

† R.C. (Remaining Content) was obtained by the difference: 100%-C(%)-H(%)-N(%)-S(%)-Ash(%).

¥ M.L. are the mass losses observed during the preparation of the materials from the precursor.

The remaining content (R.C.) in each CBA was determined from the difference of the total (100%) and the weight percentage of C, H, N, S and ash quantities. R.C. typically refers to other heteroatoms present in biomass, mainly oxygen (Diaz de Tuesta *et al.* 2021a; Diaz de Tuesta *et al.* 2018; Diaz de Tuesta *et al.* 2021b). As observed, R.C. decreased from feedstock precursors (43.6 and 42.7% for OS and MB, respectively) to hydrochars (18.5 and 23.1% for OS-HTC and MB-HTC) and pyrochars (5.8 and 11.5% for OS-P and MB-P) due to the release of species containing oxygen and other heteroatoms during carbonization processes. In HTC processes, the decrease of H and oxygen may not be evident because of the presence of water. However, H and R.C. may decrease during HTC processes due to the small fraction of gases (CO, CO_2, H_2 and CH_4) generated during the HTC process, especially when performed in temperatures below 260ºC (Basso *et al.* 2015). The same trend was observed in previous works on HTC of sugarcane bagasse (from 8.0% to 4.2-4.8% for H and from 29% to 25.9-27.2% for R.C., depending on the operational conditions) (Diaz de Tuesta *et al.* 2021a).

3.2. Textural properties of CBAs

Table 1 also summarizes the textural properties of the CBAs obtained from the analysis of the N_2 adsorption isotherms of the adsorbents (*cf*. Figure 2). The amount adsorbed of N_2 on the OS and MB carbon precursors was negligible. As observed, pyrolysis led to a considerable improvement in these properties since OS-P and MB-P show the highest values of BET surface areas (172 and 50 m^2 g^{-1} for OS-P and MB-P, respectively) and total pore volume (109 and 34 mm^3 g^{-1} for OS-P and MB-P, respectively), due to the removal of volatile matter through the pyrolysis process, that enriched the carbon composition, forming the porosity on these adsorbents (Yek *et al.* 2019). The external surface area (S_{ext}) determined from the *t*-plot method applied to each CBA adsorption isotherm was close to each other, taking values of 4, 14, 11 and 11 m^2 g^{-1} for OS-HTC, OS-P, MB-HTC and MB-P, respectively. In accordance, the hydrochars OS-HTC and MB-HTC are not microporous adsorbents (S_{mic} = 0-1 m^2 g^{-1}), whereas the pyrochars OS-P and MB-P present a significant microporous surface (158 and 39 m^2 g^{-1} for OS-P and MB-P, respectively). These materials are predominately microporous since, respectively, 76% and 59% of the pore volume consists of micropores (determined as V_{mic}/V_{Total}).

3.3. Acid-base functionalities on CBAs

Table 2 presents the values of basicity and acidity in mmol g^{-1} and in µmol m^{-2} (determined considering S_{BET}) of each CBA. The HTC process is expected to produce a material with high concentrations of surface oxygen-containing functional groups, including basic and acid ones (Jain *et al.* 2016). In this case, the hydrochars (OS-HTC and MB-HCT) are predominantly acid adsorbents and show the highest acidity values (2.34 and 2.37 mmol g^{-1}, and 585 and 198

µmol m^{-2}, respectively) among all the prepared materials, due to the use of H_2SO_4 in the HTC process. On the other hand, pyrochars (OS-P and MB-P) show higher basicity (1.10 and 0.59 mmol g^{-1}, respectively) compared to hydrochars (0.11-0.14 mmol g^{-1}) and biomass precursors (0.41-0.44 mmol g^{-1}). The highest basicity of OS-P and MB-P is ascribed to the increase in ashes content related to minerals, mainly alkali and alkaline earth metals, as explained above (Diaz de Tuesta *et al.* 2021b; Lacey *et al.* 2018; Jahn *et al.* 2020).

Table 2. Volume used during titration and acid-based properties of the carbonaceous materials prepared from olive stone (OS) and malt bagasse (MB).

CBA	V_{NaOH} (mL)	Acidity (mmol g^{-1})	SA* (µmol m^{-2})	V_{HCl} (mL)	Basicity (mmol g^{-1})	SB* (µmol m^{-2})
OS-HTC	1.3	2.34	585	19.1	0.11	27.5
OS-P	17.3	0.32	1.86	11.2	1.10	6.40
OS	8.2	1.47	-	16.7	0.41	-
MB-HTC	1.1	2.37	198	19	0.14	11.7
MB-P	17.2	0.34	6.80	15.4	0.59	11.8
MB	8.6	1.42	-	16.6	0.44	-

** SA = Acidity/S_{BET}, SB = Basicity/S_{BET}*

3.4. Removal of NH_3 with the CBAs

For the NH_3 adsorption runs, blank experiments were conducted with non-CBA bed to ensure the operational conditions, allowing a constant NH_3 concentration in the saturated air from the GWB containing leachate. Bearing this in mind, the concentration of NH_3 was monitored and all runs were conducted using an initial concentration of 9 ppm in the inlet of the bed, maintained constant for 10 h of adsorption run.

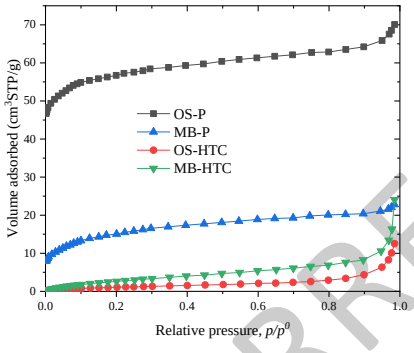

Figure 2. N_2 adsorption isotherms of CBAs prepared from olive stone and malt bagasse.

Figure 3 shows breakthrough curves obtained in the NH_3 adsorption runs carried out with each CBA, whereas experimental data obtained from the curves are summarized in Table 3.

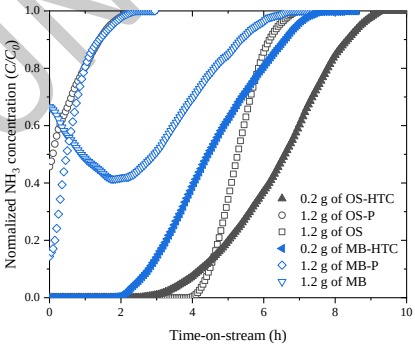

Figure 3. Breakthrough curves obtained in the NH_3 adsorption runs with each CBA at room temperature, 0.8 mL min^{-1} and the load of CBA in the adsorption bed shown in the figure.

As observed, half of the CBAs (MB, OS-P and MB-P) were unable to adsorb completely the inlet concentration of NH_3 at the beginning of the experiments, thus being not possible to observe the breakthrough curves at the selected operational conditions, due the fact that adsorption of NH_3 does not have a significant mass transfer barrier for those CBAs (Chou *et al.* 2006). On the other hand, the monitoring of the adsorption of NH_3 on 1.2 g of hydrochars (OS-HTC and MB-HCT) was not possible, owing to the large breakthrough time (t_h > 12 h) needed with these CBAs, because of the highest uptake capacity of the hydrochars. Accordingly, the NH_3 adsorption runs on both hydrochars (OS-HTC and MB-HCT) were repeated using lower loads of material in the bed (0.2 g) than those used for other CBAs (1.2 g), determining the uptake capacity of OS-HTC and MB-HTC in 10.4 and 7.2 mg g^{-1}, respectively. The value of Q_a was considerably higher than those obtained with pyrochars (0.07-0.21 mg g^{-1}) and 8 to 10 times higher than the value obtained with the biomass precursor (0.43-1.22 mg g^{-1}) using 1.2 g on the adsorption bed. To the best of our knowledge, similar values have been reported in only one paper (Huang *et al.* 2008), in which commercial coconut shell AC treated with H_2SO_4 shows an uptake capacity between 7.49 and 11.25 mg g^{-1}. The values of Q_a with the hydrochars were higher than the uptake capacity reported with commercial adsorbents: (0.6–1.8 mg g^{-1}) (Rodrigues *et al.* 2007), (4.7–5.3 mg g^{-1}) (Gonçalves *et al.* 2011) and (2.3 mg g^{-1}) (Huang *et al.* 2008). Additionally, the hydrochars prepared in this work show a low H_{MTZ}/Z which means that their mass transfer front takes longer to reach the exit of the column (t_b of 5.0 – 3.3 h was observed). However, as the hydrochars OS-HTC and MB-HTC show very low values for the textural parameters (*cf.* Table 1), the highest uptake capacities of these CBAs may be explained by the presence of acidic groups that give a polar character to the surface of the hydrochars, affecting the preferential adsorption of polar alkaline adsorbates, being such groups considered the key factor on the values of Q_a obtained (Gonçalves *et al.* 2011; Foo *et al.* 2013), concluding that the development of porosity is not so important for the adsorption of NH_3, as is the acidity of the surface.

According to ASTM International (2019), the best adsorbent for most applications should have a high Q_a coupled with a short H_{MTZ}. Therefore, the hydrochar

prepared from olive stones (OS-HTC) was the best adsorbent for NH_3 removal produced in this work since it has shown a low H_{MTZ} per height of bed (H_{MTZ}/Z = 56%) and the highest Q_a (10.4 mg g^{-1}).

It is noteworthy to note that the precursors (OS and MB) were able to adsorb NH_3, showing a greater Q_a than the pyrochars OS-P and MB-P prepared from those precursors, likely due to the highest acidity of the precursors (1.42–1.47 mmol g^{-1} of acidity) compared to the pyrochars (0.32–0.34 mmol g^{-1} of acidity). Among the precursors, OS shows the highest Qa (1.22 mg g^{-1}) and the shorter HMTZ/Z (33%), evidencing that it is expectable to obtain better hydrochars from acid precursors with high uptake capacities. Considering its properties, OS adsorbent may be used as an effective CBA for NH_3 removal since similar values of t_b, t_{sto}, t_{sat} than those obtained with OS-HTC were observed, however with an adsorption bed load six times higher than that used with the hydrochar OS-HTC.

Table 3. Breakthrough time (t_b), stoichiometric time (t_{sto}), saturation time (t_{sat}), height of mass transfer zone per height of the adsorption bed (H_{MTZ}/Z), and dynamic adsorption capacity (Q_a) obtained in the adsorption runs of gaseous NH_3 on each CBA at room temperature, 0.8 mL min^{-1} and the mass of adsorbent (m_{CBA}) and void fraction of bed ($Void_f$) shown in Table.

Adsorbent	t_b (h)	t_{sto} (h)	t_{sat} (h)	H_{MTZ}/Z (%)	Q_a (mg g^{-1})	m_{CBA} (g)	$Void_f$ (%)
OS-HTC	3.8 (±1.3)	6.6 (±1.0)	8.7 (±0.8)	56	10.4 (±1.0)	0.2	20
OS-HTC	>12	-	-	-	-	1.2	20
OS-P	-	-	1.7 (±0.1)	-	0.07 (±0.01)	1.2	10
OS	4.3 (±0.4)	5.3 (±0.5)	6.4 (±0.5)	33	1.2 (±0.2)	1.2	50
MB-HTC	2.4 (±0.5)	4.4 (±0.6)	6.9 (±0.2)	65	7.2 (±0.9)	0.2	30
MB-HTC	>12	-	-	-	-	1.2	30
MB-P	-	-	1.8 (±0.1)	-	0.21 (±0.01)	1.2	10
MB	-	-	-	-	0.43 (±0.01)	1.2	75

3.5. The regeneration of OS and OS-HTC

Taking into account the performance of both OS and OS-HTC, these materials were regenerated and reused in a second cycle of NH_3 adsorption at the same operational conditions. The regeneration of OS and OS-HTC was conducted by washing the CBAs with ultrapure water to desorb NH_3, which is a compound highly soluble in water (Ro *et al.* 2015). Afterwards, washed CBAs were dried at 100ºC overnight and considered ready for a 2nd cycle.

Figure 4 presents the breakthrough curves obtained in the NH_3 adsorption runs carried out with the regenerated OS and OS-HTC and Table 4 summarizes their parameters. It is noticed that the regenerated OS and OS-HTC show t_b, t_{sto}, t_{sat} and Q_a lower than the mean values of the same parameters of the first-generation samples (the values of the parameters decrease 16-35%). The less performance is due to the lowest acidity of the regenerated CBAs (1.95 and 1.43 mmol g^{-1} for regenerated OS-HTC and OS, respectively, which is 3-17% lower than the values of OS-HTC and OS prior to its first use).

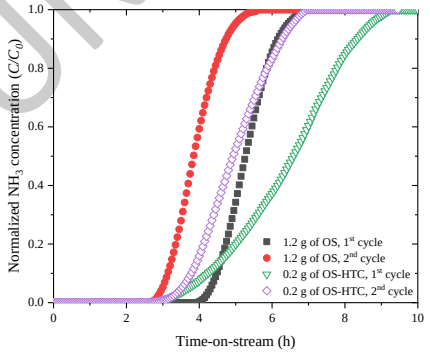

Figure 4. Breakthrough curves obtained in the NH_3 adsorption runs with OS and OS-HTC after recovered, washed and reused at room temperature, 0.8 mL min^{-1} and the adsorption bed load of CBA shown in the Figure.

This means that CBAs may be easily recycled by washing with water at mild conditions (room temperature was tested in this work). In addition, the regenerated OS-HTC shows a lower $H_{MTZ/Z}$ (45%) than the samples in its first use (56%), suggesting that the adsorption process on the water-washed OS-HTC does not show a significant mass transfer barrier.

4. Conclusions

The feasibility for the preparation of different carbon-based adsorbents (CBAs) from two biomass residues coming from agro-industrial exploration (olive stone and malt bagasse) has been proved, showing that biomass residues can be valorized into high-added-value products with environmental applications to reach a suitable circular economy. In this work, H_2SO_4-assisted hydrothermal carbonization (HTC) and pyrolysis were assessed for the preparation of hydrochars and pyrochars with different acid-based and textural properties, which were tested in the treatment of a gaseous NH_3 derived from a leachate obtained in a mechanical and biological treatment unit of municipal solid waste.

The CBAs showing the highest uptake capacity were those prepared by HTC since those samples show a high acidity, which is required for a great performance in the removal of NH_3. In fact, pyrochar shows higher development of porosity than hydrochars, but lower acidity making them more inefficient for the adsorption of NH_3. In this sense, H_2SO_4-assisted hydrothermal carbonization confers highlighted acidity and uptake capacity to the CBAs. In addition, the regeneration of the hydrochars is available through washing with water.

Author contributions

Thalles P. Lima: Investigation, Formal analysis, Writing - Original draft preparation. Jose L. Diaz de Tuesta: Methodology, Formal analysis, Visualization, Supervision, Writing - Original draft preparation, Writing - Review & Editing, Funding acquisition.

Manuel Feliciano: Supervision, Writing - Review & Editing, Conceptualization, Funding acquisition. Leonardo Campestrini Furst: Investigation. Fernanda Roman: Investigation. Adriano S. Silva: Investigation. Adriana A. Pereira Wilken: Supervision. Adrián M.T. Silva: Supervision, Writing - Reviewing and Editing. Helder T. Gomes: Supervision, Writing - Reviewing and Editing, Funding acquisition.

Acknowledgements

The authors thank the Base Funding UIDB/00690/2020 of the *Centro de Investigação de Montanha* (CIMO) - funded by national funds through FCT/MCTES (PIDDAC); and the scientific collaboration under Base-UIDB/50020/2020 and Programmatic-UIDP/50020/2020 Funding of LSRE-LCM - funded by national funds through FCT/MCTES (PIDDAC). Jose L. Diaz De Tuesta acknowledges the financial support through the program of *Atracción al Talento* of *Comunidad de Madrid* (Spain) for the individual research grants 2020-T2/AMB-19836 and 2022-T1/AMB-23946. Fernanda F. Roman and Adriano dos Santos Silva acknowledge the national funding by FCT and the European Social Fund, FSE, for individual research grants with reference numbers of SFRH/BD/143224/2019 and SFRH/BD/151346/2021, respectively.

References

Ang T.N., Young B.R., Taylor M., Burrell R., Aroua M.K. and Baroutian S. (2020), Breakthrough analysis of continuous fixed-bed adsorption of sevoflurane using activated carbons, *Chemosphere*, **239**, 124839.

Baldikova E., Mullerova S., Prochazkova J., Rouskova M., Solcova O., Safarik I. and Pospiskova K. (2019), Use of waste *Japonochytrium* sp. biomass after lipid extraction as an efficient adsorbent for triphenylmethane dye applied in aquaculture, *Biomass Conversion and Biorefinery*, **9(3)**, 479–488.

Balsamo M., Rodríguez-Reinoso F., Montagnaro F., Lancia A. and Erto A. (2013), Highlighting the role of activated carbon particle size on CO_2 capture from model flue gas, *Industrial & Engineering Chemistry Research*, **52(34)**, 12183–12191.

Basso D., Weiss-Hortala E., Patuzzi F., Castello D., Baratieri M. and Fiori L. (2015), Hydrothermal carbonization of off-specification compost: A byproduct of the organic municipal solid waste treatment, *Bioresource Technology*, **182**, 217–224.

Bi Z., Kong Q., Cao Y., Sun G., Su F., Wei X., Li X., Ahmad A., Xie L. and Chen C.-M. (2019), Biomass-derived porous carbon materials with different dimensions for supercapacitor electrodes: a review, *Journal of Materials Chemistry A*, **7(27)**, 16028–16045.

Cagnon B., Py X., Guillot A., Stoeckli F. and Chambat G. (2009), Contributions of hemicellulose, cellulose and lignin to the mass and the porous properties of chars and steam activated carbons from various lignocellulosic precursors, *Bioresource Technology*, **100(1)**, 292–298.

Chen Y., Zhang X., Chen W., Yang H. and Chen H. (2017), The structure evolution of biochar from biomass pyrolysis and its correlation with gas pollutant adsorption performance, *Bioresource Technology*, **246**, 101–109.

Cheng Z., Sun Z., Zhu S., Lou Z., Zhu N. and Feng L. (2019), The identification and health risk assessment of odor emissions from waste landfilling and composting, *Science of The Total Environment*, **649**, 1038–1044.

Chou L.H., Tsai R.I., Chang J.R. and Lee M.T. (2006), Regenerable adsorbent for removing ammonia evolved from anaerobic reaction of animal urine, *Journal of Environmental Sciences*, **18(6)**, 1176–1181.

Dai Y., Sun Q., Wang W., Lu L., Liu M., Li J., Yang S., Sun Y., Zhang K., Xu J., Zheng W., Hu Z., Yang Y., Gao Y., Chen Y., Zhang X., Gao F. and Zhang Y. (2018), Utilizations of agricultural waste as adsorbent for the removal of contaminants: A review, *Chemosphere*, **211**, 235–253.

de Freitas Batista G., Roman F.F., de Tuesta J.L.D., Mambrini R.V., Praça P. and Gomes H.T. (2022), Assessment of pretreatments for highly concentrated leachate waters to enhance the performance of catalytic wet peroxide oxidation with sustainable low-cost catalysts, *Catalysts*, **12(2)**, 238.

Diaz de Tuesta J.L., Silva A.M.T., Faria J.L. and Gomes H.T. (2018), Removal of Sudan IV from a simulated biphasic oily wastewater by using lipophilic carbon adsorbents, *Chemical Engineering Journal*, **347**, 963–971.

Diaz de Tuesta J.L., Saviotti M.C., Roman F.F., Pantuzza G.F., Sartori H.J.F., Shinibekova A., Kalmakhanova M.S., Massalimova B.K., Pietrobelli J.M.T.A., Lenzi G.G. and Gomes H.T. (2021a), Assisted hydrothermal carbonization of agroindustrial byproducts as effective step in the production of activated carbon catalysts for wet peroxide oxidation of micro-pollutants, *Journal of Environmental Chemical Engineering*, **9(1)**, 105004.

Diaz de Tuesta J.L., de Almeida F.V.M., Oliveira J.R.P., Praça P., Guerreiro M.C. and Gomes H.T. (2021b), Kinetic insights on wet peroxide oxidation of caffeine using EDTA-functionalized low-cost catalysts prepared from compost generated in municipal solid waste treatment facilities, *Environmental Technology & Innovation*, **24**, 101984.

Foo K.Y., Lee L.K. and Hameed B.H. (2013), Preparation of activated carbon from sugarcane bagasse by microwave assisted activation for the remediation of semi-aerobic landfill leachate, *Bioresource Technology*, **134**, 166–172.

Franciski M.A., Peres E.C., Godinho M., Perondi D., Foletto E.L., Collazzo G.C. and Dotto G.L. (2018), Development of CO_2 activated biochar from solid wastes of a beer industry and its application for methylene blue adsorption, *Waste Management*, **78**, 630–638.

Ghouma I., Jeguirim M., Dorge S., Limousy L., Matei Ghimbeu C. and Ouederni A. (2015), Activated carbon prepared by physical activation of olive stones for the removal of NO_2 at ambient temperature, *Comptes Rendus Chimie*, **18(1)**, 63–74.

Gonçalves M., Sánchez-García L., Oliveira Jardim E., Silvestre-Albero J. and Rodríguez-Reinoso F. (2011), Ammonia removal using activated carbons: effect of the surface chemistry in dry and moist conditions, *Environmental Science & Technology*, **45(24)**, 10605–10610.

González J.F., Román S., Encinar J.M. and Martínez G. (2009), Pyrolysis of various biomass residues and char utilization for the production of activated carbons, *Journal of Analytical and Applied Pyrolysis*, **85(1–2)**, 134–141.

Hadi P., Xu M., Ning C., Sze Ki Lin C. and McKay G. (2015), A critical review on preparation, characterization and utilization of sludge-derived activated carbons for wastewater treatment, *Chemical Engineering Journal*, **260**, 895–906.

Huang C.-C., Li H.-S. and Chen C.-H. (2008), Effect of surface acidic oxides of activated carbon on adsorption of ammonia, *Journal of Hazardous Materials*, **159(2–3)**, 523–527.

Jahn L.G., Polen M.J., Jahl L.G., Brubaker T.A., Somers J. and Sullivan R.C. (2020), Biomass combustion produces ice-active minerals in biomass-burning aerosol and bottom ash., *Proceedings of the National Academy of Sciences*, **117(36)**, 21928–21937.

Jain A., Balasubramanian R. and Srinivasan M.P. (2016), Hydrothermal conversion of biomass waste to activated carbon with high porosity: a review, *Chemical Engineering Journal*, **283**, 789–805.

Karimi M., Diaz de Tuesta J.L., d. P. Gonçalves C.N., Gomes H.T., Rodrigues A.E. and Silva J.A.C. (2020), Compost from municipal solid wastes as a source of biochar for CO_2 capture, *Chemical Engineering & Technology*, **43(7)**, 1336–1349.

Lacey J.A., Aston J.E. and Thompson V.S. (2018), Wear properties of ash minerals in biomass, *Frontiers in Energy Research*, **6**, 119.

Lam S.S., Liew R.K., Wong Y.M., Yek P.N.Y., Ma N.L., Lee C.L. and Chase H.A. (2017), Microwave-assisted pyrolysis with chemical activation, an innovative method to convert orange peel into activated carbon with improved properties as dye adsorbent, *Journal of Cleaner Production*, **162**, 1376–1387.

Martín-Lara M.A., Blázquez G., Ronda A., Pérez A. and Calero M. (2013), Development and characterization of biosorbents to remove heavy metals from aqueous solutions by chemical treatment of olive stone, *Industrial & Engineering Chemistry Research*, **52(31)**, 10809–10819.

Mello L.R.P.F. and Mali S. (2014), Use of malt bagasse to produce biodegradable baked foams made from cassava starch, *Industrial Crops and Products*, **55**, 187–193.

Mohamed A.R., Mohammadi M. and Darzi G.N. (2010), Preparation of carbon molecular sieve from lignocellulosic biomass: a review, *Renewable and Sustainable Energy Reviews*, **14(6)**, 1591–1599.

Nicell J.A. (2009), Assessment and regulation of odour impacts, *Atmospheric Environment*, **43**, 196–206.

Rincón C.A., De Guardia A., Couvert A., Le Roux S., Soutrel I., Daumoin M. and Benoist J.C. (2019), Chemical and odor characterization of gas emissions released during composting of solid wastes and digestates, *Journal of Environmental Management*, **233**, 39–53.

Ro K., Lima I., Reddy G., Jackson M. and Gao B. (2015), Removing gaseous NH_3 using biochar as an adsorbent, *Agriculture*, **5(4)**, 991–1002.

Rodrigues C.C., de Moraes Jr D., Danobrega S.W. and Barboza M.G. (2007), Ammonia adsorption in a fixed bed of activated carbon, *Bioresource Technology*, **98(4)**, 886–891.

Roman F.F., Diaz de Tuesta J.L., Silva A.M.T., Faria J.L. and Gomes H.T. (2021a), Carbon-based materials for oxidative desulfurization and denitrogenation of fuels: a review, *Catalysts*, **11(10)**, 1239.

Roman F.F., Diaz de Tuesta J.L., Praça P., Silva A.M.T., Faria J.L. and Gomes H.T. (2021b), Hydrochars from compost derived from municipal solid waste: Production process optimization and catalytic applications, *Journal of Environmental Chemical Engineering*, **9(1)**, 104888.

Santos Silva A., Seitovna Kalmakhanova M., Kabykenovna Massalimova B., G. Sgorlon J., Jose Luis D. de T. and T. Gomes H. (2019), Wet peroxide oxidation of paracetamol using acid activated and Fe/CO-pillared clay catalysts prepared from natural clays, *Catalysts*, **9(9)**, 705.

Susanti R.F., Arie A.A., Kristianto H., Erico M., Kevin G. and Devianto H. (2019), Activated carbon from citric acid catalyzed hydrothermal carbonization and chemical activation of salacca peel as potential electrode for lithium ion capacitor's cathode, *Ionics*, **25(8)**, 3915–3925.

Vieira O., Ribeiro R.S., Diaz de Tuesta J.L., Gomes H.T. and Silva A.M.T. (2022), A systematic literature review on the conversion of plastic wastes into valuable 2D graphene-based materials, *Chemical Engineering Journal*, **428**, 131399.

Yek P.N.Y., Liew R.K., Osman M.S., Lee C.L., Chuah J.H., Park Y.-K. and Lam S.S. (2019), Microwave steam activation, an innovative pyrolysis approach to convert waste palm shell into highly microporous activated carbon, *Journal of Environmental Management*, **236**, 245–253.

Zafanelli L.F.A.S., Henrique A., Steldinger H., Diaz de Tuesta J.L., Gläsel J., Rodrigues A.E., Gomes H.T., Etzold B.J.M. and Silva J.A.C. (2022), 3D-printed activated carbon for post-combustion CO_2 capture, *Microporous and Mesoporous Materials*, **335**, 111818.

Zhang Z., Zhu Z., Shen B. and Liu L. (2019), Insights into biochar and hydrochar production and applications: A review, *Energy*, **171**, 581–598.